

# Natural Rock's Minerals: Non Isothermal and Heat flow Analysis

C.M.Patel<sup>1</sup> & C.D.Patel<sup>1</sup>

<sup>1</sup>Department of Physics, Faculty of Science, Sankalchand Patel University, Visnagar, Gujarat 384002, India

Date of Submission: 15-12-2020

Date of Acceptance: 30-12-2020

**ABSTRACT:** The rocks minerals obtain from different region contain different nature, properties and applications. The Rock mineral such as calcite, china clay, talc and whitening in the form of rock specimen collected from different part of Rajasthan. The final materials in the form of powder in micrometer size were obtained using mechanical method. In the current paper, the dynamic temperature aspect was well thought-out eventually and concluded the results in respective section. The DSC measurements curve illustrates heat flow with rising temperature. Specific heat capacities and thermal diffusivities of rock's minerals were measured from the analytical data. The investigation peak and region corresponds to enthalpy involves in the process identified in schematic DSC curve. Present investigation deals with measurement of the enthalpy of fusion, enthalpy of crystallization and melting point of minerals besides of some other thermal event measurement briefly discussed at room temperature to decomposition temperature. The authors carried out the measurement and calculation with all the scientific evidence. Phase transitions, transition due to resultant energy changing as well as glass transitions also recognized and discussed.

**Keywords:** Heat Flow, Thermal diffusivities, Thermal Transition, Specific heat, Phase Transition.

## I. INTRODUCTION

Mineral raw materials are extensively used for more or less complex ceramic compositions since times in a large range of possible applications with particular characteristics of ceramic materials are often affected by the existence of micro-composite microstructures with a crystalline phase embedded in a silico-alumina matrix[1]. Rock minerals namely talc, calcite, china clay, whitening, and mica are common for used in highly commercialized thermoplastic material which is used in a range of applications including packaging, paint appliances, consumer electronics, construction, medical and various other uses. They are associated with minor amounts of chlorites, dolomites, calcites, magnetite and quartz[2], in compositions and concentrations which depend on the processing of the mineral. The

influence of these mineral impurities in the mechanical, thermal and electrical behavior of the talc composites is an important issue. Consequently, the characterization of the different composites minerals is a necessary task for the fabrication of talc composites[3].

For the last two decades, one of the rapidly growing areas for the use of raw materials for Solvent. This is due to convenience, safety, low price and good aesthetic qualities of composition of Pigment. Continuing research efforts have been devoted to the development of composites which can be used as the binder to hold the pigment particles together and provide adhesion to the surface painted. Various methods based on simple mechanical mixing, bulk polymerization, solution polymerization and emulsion polymerization have been employed. Calcium carbonate (CaCO<sub>3</sub>) in the form of chalk, whiting, and limestone is the most commonly used inorganic filler in thermoplastics, such as polypropylene[4] among the approaches mentioned above, emulsion polymerization is more attractive for the ease of manipulation, low cost and environmental friendliness[5-6]. In the area of mineral raw materials, we must consider firstly calcite, china clay, talc and whitening. This mineral is often used, for its enough properties and because it enters in the mineralogical composition of many suitable clays for ceramics.

The current research focuses on the synthesis and characterization of various minerals composite materials with improved mechanical and thermal properties to be used as construction material, abrasive, agricultural soil treatment, construction aggregate, pigment, pharmaceutical and more. To date, a large number of research works have been carried out on the energy minerals, metals, construction minerals and industrial minerals. Energy minerals are used to produce electricity, fuel for transportation, heating for homes and offices and in the manufacture of plastics[6-7]. Kaolinite is one of the most common clay minerals found on the Earth's crust. It is widely used in several engineering applications and in different industrial sectors such as the ceramic industry, and the manufacturing of paper,

potteries, paints, and cosmetics, as well as a sorbent for pollutants[8-9]

Differential scanning calorimetry(DSC) is an effective analytical tool to characterize the physical properties of a ceramic material. DSC enables the measurements of the transition such as the glass transition, melting, and crystallization. Furthermore, the chemical reaction such as thermal curing, heat history, specific heat capacity, and purity analysis are also measurable. Heat flow is proportional to the heat difference of heat sink and holders. Heat sink has the enough heat capacity compared to the sample. Specific heat capacity is the most useful quantity available from DSC, because it is directly related to sample properties and, according[10-13] the structure and composition of Calcite, China Clay, Talc, and Whiting are studied as samples change during heating. These changes of curve are determining all physical properties of the samples, including thermophysical properties[14-18]. In general, the results of the heat capacity reveal the processes in the samples which are linked with the consumption and release of heat which are represented as maxima and minima in the enthalpy curve, respectively.

The silicates are more abundant, although non-silicates are very common as well. Not only do the two exhibit differences in their composition but also in their structure. The structure of silicates tends to be more complex, while the structure of non-silicates features a great deal of variability[19-20]. This fact can be attributed to the intrinsic degradation of the  $\text{CaCO}_3$  particles and their large surface area, such that even at lower loadings of fillers they are effective to transfer the heat through the samples[20-21].

## II. REVIEW OF LITERATURE

Talc, China Clay and Whiting thermal kinetic curve with three different stages, namely: an initial rapid stage of uranium adsorption, a stage with the rippling effect of adsorption/desorption processes and the third stage of adsorption slowly approaching to equilibrium[22].

The kinetic behavior of the oil shale polypropylene mixture is degradation with first-order reaction was indicated by the results of the isoconversion method as well as activation energy of organic matter decomposition of the mixture is 242 kJ mol<sup>-1</sup>, substantially higher than that for the unmixed oil shale (63 kJ mol<sup>-1</sup>) and close to that of polypropylene (250 kJ mol<sup>-1</sup>)[23].

Thermogravimetric analysis of sago starch film and the two sago starch nanocomposites revealed reduced thermal stability of the starch matrix in the presence of nanoparticles. Also, the activation energies of the main degradation process

of the nanocomposites are lower than that of pure starch as calculated using Horowitz-Metzger and Broido methods[24].

The heat capacity contribution of the substance that evaporates can also be subtracted, since the actual instantaneous weight of the substance that evaporates can be obtained from the TGA trace with calculation of specific heat flow of the sample, less the total effect of the substance that evaporates, can be performed by combining the corrected heat flow with the actual mass of the remaining sample[25].

## III. EXPERIMENTAL MATERIAL AND METHODS

### 1) Materials and Sample Preparation

The main objective of this investigation was to study and compare the thermal rigidity, thermal stability, and process ability for various minerals like Calcite, China Clay, Talc and whiting which are taking at different area in Rajasthan. A lumps of material (Calcite, China Clay, talc and whiting) was crushed in Jew Curser and obtain powders in micro size in between 10 to 100  $\mu\text{m}$  were separated from the powdered material according to Stokes's law. Moisture in a weighted sample is removed by heating in an oven under specified conditions of time at H.N.G.U laboratory, Patan.

### 2) Specific Heat Treatment

Specific heat capacity and Heat flow measurements were performed using a modulated differential scanning calorimeter DSC Mettler-Toledo DSC-1 STARE SYSTEM at Charotar University of Science and Technology, Changa, Gujarat. DSC measurements were carried out under dynamic non-isothermal conditions and in a flow of extra-pure nitrogen gas atmosphere in the temperature range of 25-1000°C, and the scanning rate was 10°C/min. The DSC was calibrated in the same temperature region before each experiment, using a sapphire sample as standard, with a well-known specific heat capacity. This leads to an accuracy of  $\pm 2\%$  for the presented data with complementary DSC heat flow sensor simultaneously detects thermal events such as melting and crystallization in addition to providing accurate and precise transition temperatures.

On the basis of the DSC experimental result reveal two types underneath peak and one overhead peak. The first underneath peak called endothermic peak in the temperature range 25-250°C represents the liberation of physically bound water from the pores and surfaces called as glass transition of minerals. The second endothermic peak represents

the decomposition of given materials which runs as function of temperature and is accompanied by the mass loss which is established by TGA plot. This endothermic peak attributed to euphemize more heat energy which is known as melting point. The area of heat absorption at constant pressure and volume is described as enthalpy of fusion ( $\Delta H_f$ ). Accurate enthalpy ( $\Delta H$ ) of minerals may be derived through carefully extrapolated heat capacity functions. The third aloft peak is determining exothermic peak due to crystallization of compound. The temperature region where the crystallization occurs is described in form as area by enthalpy of crystallization ( $\Delta H_C$ ).

#### IV. RESULTS AND DISCUSSION

##### 1) Non-Isothermal Heat Flow

The DSC measurement of heat flow can be performed as dynamically using non isothermal linear temperature. The experimental result of DSC deposited curve for all four minerals shown in figure 1 such as plot of heat flow  $Q$  (mW) vs reference temperature  $Tr$  ( $^{\circ}C$ ). Additionally the derivative curve of heat flow deposits also as well as a derivative curve reveals accurate temperature when occurring thermal event. It is clearly shows two or three peaks occur at various temperatures. These various peaks reveal thermal event such as glass transition, crystallization and melting behavior of minerals, according to [26]. The first heating curve tells about processing of minerals where as second heating curve is important natural characteristics. The glass transition is not very prominent due to enthalpy relaxations such as calcite minerals does not occur glass transition but china clay, talc and whiting minerals occur in temperature range of 25-250 $^{\circ}C$  with a derivative curve of china clay, talc and whiting reveal small endothermic peak shown as fig. 1. The second endothermic peak is occurring in all four minerals attributes to melting behaviour.

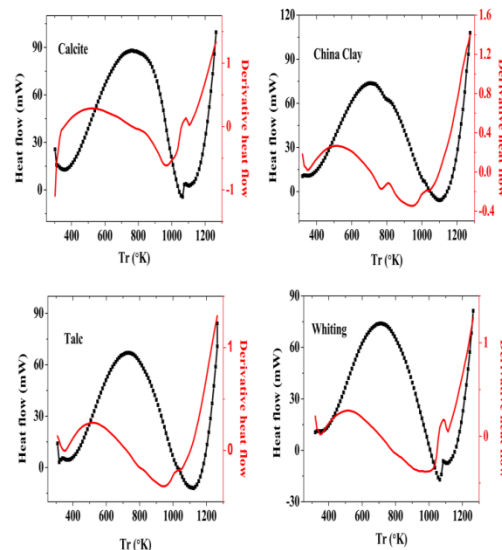


**Fig. 1.** The Plot of Heat Flow & Derivative Heat Flow versus Reference Temperature of Calcite, China Clay, Talc and Whiting.

For calcite minerals present investigation heat flow curve with reference temperature illustrated in fig. 1. Form calcite plot at 1000 $^{\circ}C$  heat flow reached at ~115 (mW). Curve has influence two peak during heating treatment of calcite, it can see by derivative heat flow curve. The first down peak as compeer ideal way occurs at ~684 $^{\circ}K$  due to calcite ( $CaCO_3$ ) split in to  $CaO$  and  $CO_2$ , this event absorbs heat and reaction process is known as endothermic respectively [27]. The second peak is occurring at 812 $^{\circ}C$  with higher temperature as compare to first peak. This peak is attributing to crystallization of  $CaO$  with accompanied uniformly mass loss with 28.8 % (from TGA analysis) which is known as endothermic reaction [28].

According to derivative heat flow curve China clay and talc has occurring three peaks during heat treatment at 1000 $^{\circ}C$  shown in fig. 1. China clay and talc has occurred first peak in temperature interval 25-200 $^{\circ}C$ . The first peak represents process of dehydration, which is an endothermic reaction, where the liberation of physically bound water occurs. The second significance peak corresponds to dehydroxylation of China Clay where a structure transformation of china clay (kaolinite) to metakaolinite and chemically bound water evaporates as well as during the heating of talc mineral, water is liberated in distinct steps due to differences in its bonding energy. This underneath peak due to the loss of the adsorption water occurs at 487 $^{\circ}C$ . This reaction is also endothermic where third peak is exothermic and represents transformation of metakaolinite into Al-Si spinel [29]. On the other

hand, the third peak for talc minerals is occur at higher temperatures 742°C can be ascribed to usually the crystallization of silica as cristobalite, and crystallization of magnesium metasilicate which is known as exothermic effects. The first is endothermic peak corresponding with dehydration so, physically bound water evaporates from pores and surface of crystals[30]. The second peak is also endothermic and reaction begins above 800°C when the structure of clinoptilolite is definitely destroyed and amorphous phase is formed[31].

Heat treatment for whiting mineral, obtain curve with increasing temperature up to 1000°C which is shown in fig. 3. The derivative heat flow curve clearly shows whiting has three peaks influence at various temperature. The first small peak occurs in temperature interval 25-150°C. This lower temperature peak represents the decomposition of the whiting structure, releasing carbon dioxide from the carbonate ion associated with magnesium part of the structure accompanied by the formation of calcite and magnesium oxide. This event is representing as glass transition. The second significance underneath peak occurs at 811°C due to heat absorbance reveals strong endothermic effect due to dehydroxylation and at 841°C the second peak observed which is attributing to exothermic reaction[32].

## 2) Measurements Of Thermal Parameter

In present DSC analysis we measured the heat capacity  $C_p$  and kinetically hindered components of the response according to according to

$$dQ/dt = C_p \cdot dT/dt + f(t, T) \dots\dots\dots (1)$$

where,  $dQ/dt$  is the total heat flow,  $dT/dt$  is the temperature scanning rate with  $C_p \cdot dT/dt$  representing the reversing signal and  $f(t, T)$  is a function of time and temperature signifying kinetically controlled thermal events such as the enthalpy relax- action process which appears in the non-reversing signal[33].

The heat capacity obtained from above equation at constant pressure for all four minerals comparison has been calculated in linearly increasing temperate range 25 to 1000°C, which is illustrated as plot of heat capacity vs reference temperature shown in fig. 2. During the analysis at particular temperature period the curve has influence thermal event[3]. Those events occurring on significant temperature area which is describe as either enthalpy of fusion ( $\Delta H_f$ ) or enthalpy of crystallization ( $\Delta H_C$ ). Those plots also describe a change of enthalpy for both events either exothermic or endothermic for all four minerals. The small area below the black line depicts as brown strait line which is demonstrates either the compound melting or during this event enthalpy changes as respect to ideal way. Besides of

deep curve is also indicating the heat absorbance as function of temperature. Similar the overhead peak as compare ideally continues curve is due to crystallization. In the plot the small area of upper peak above the black line describe as straight green line indicates either the compound change in form or phase transition.

The heat capacity curves with rising temperature up to 1000°C of calcite minerals illustrate shows fig. 2. The curve is distracting in temperature interval 750-850°C due to occurring some thermal event. In the calcite curve the first peak reveal melting point attribute to fusion of compound. The  $C_p$  curve is clearly shows first event begins at 771°C ( $T_i$ ) and ends at 781°C in that interval the enthalpy of fusion ( $\Delta H_f$ ) obtain 32 J/g. The emanate peak at 790°C known as melting point and this thermal event attributes to decomposition of calcite minerals which is relevant to endothermic peak also. The second thermal event begins at 797°C and ends at 831°C ( $T_f$ ) which is associated with silicate part of the structure accompanied by the formation of calcium dioxide and carbon oxide. During this crystallization process the enthalpy of crystallization ( $\Delta H_C$ ) is 28 J/g shows in fig. 4 and at 1000°C heat capacity  $C_p$  reached  $\sim 144$  ( $Jg^{-1}C^{-1}$ ).

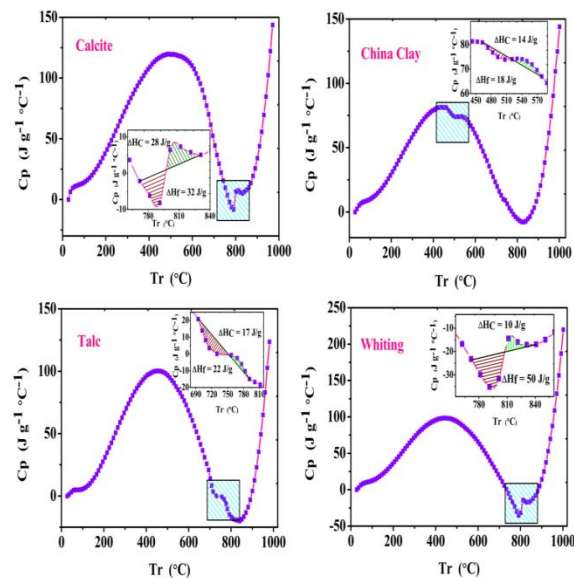


**Fig. 2.** The plot of Heat capacity versus Reference temperature as well as enthalpy of fusion ( $\Delta H_f$ ) and enthalpy of crystallization ( $\Delta H_C$ ) obtain by area of heat flow within temperature of pyrolysis of calcite, china clay, talc and whiting.

China clay minerals that heat capacity  $C_p$  curve changes as compare to ideally way in between 463-580°C. From the china clay  $C_p$  plot the first significance down peak begins at 463°C ( $T_i$ ), reaches



a peak at 494°C and ends at 518°C shows in fig. 2, attributes to fusion of china clay minerals and reveals melting point ~494°C. In this area the enthalpy of fusion ( $\Delta H_f$ ) is 18 J/g. The second peak occurs at temperature ~518°C, ends at 580°C(Tf) can be attributed to the collapse of the metakaolinite lattice and the subsequent formation of spinel[28]. The value of crystallization formation area is described as enthalpy of crystallization ( $\Delta H_c$ ) is 14 J/g shown in fig. 2. The figure obtain at 1000°C heat capacity Cp reached ~145 (Jg-1°C-1) also. Various thermal parameters with certain events displayed in table 1.

According to heat capacity curve for talc minerals that the heat capacity Cp is reached ~125 (Jg-1°C-1) at 1000°C accompanied reveals thermal event with two peaks in between 690-810°C. The first event begins at 695°C (Ti), reaches a peak at 717°C which is melting point and ends at 756°C. This reaction reveals 22 J/g enthalpy of fusion ( $\Delta H_f$ ) attribute to degradation of the talc structure by Krupka,et al. (1985)[34]. The second peak begins at 756°C and ends at 792°C (Ti) with formation of the crystalline cristobalite and magnesium metasilicate from the amorphous decomposition products of the mineral by Wesolowski et al. (1984)[35]. During this

crystallization process enthalpy of crystallization ( $\Delta H_c$ ) obtain 17 J/g shows fig. 2 and at end of experiment at 1000°C heat capacity reached ~125 (Jg-1°C-1).

The curve of whiting minerals at 1000°C value of heat capacity reached ~219 (Jg-1°C-1) shown in fig. 2 accompanies in between 750-870°C thermal event observed also. The first underneath peak observed at ~770°C(Ti) with begins thermal event either endothermic or exothermic, reached at ~795°C with minimums heat capacity around -40 (Jg-1°C-1) knows as melting point due to fusion of material such as in this interval during the fusion obtain enthalpy of fusion ( $\Delta H_f$ ) is 50 J/g shows fig. 2. This endothermic reaction occurs due to either heat observed or decomposition of the whiting structure[36]. The upper peak as compare to ideal way observed at ~808°C and ends at ~840°C (Tf). This thermal event associated with magnesium part of the structure accompanied by the formation of calcite and magnesium oxide[37]. This crystallization obtain as enthalpy of crystallization ( $\Delta H_c$ ) is 10 J/g. after that at 1000°C heat capacity reached ~225 (Jg-1°C-1) shows in fig. 2.

**Table 1.** Some parameter of thermal event with certain temperature.

Minerals	Melting range		Enthalpy of Fusion $\Delta H$ (J/g)	Specific heat Capacity at Ti Cp (J g-1 °C-1)	Enthalpy of crystallization ( $\Delta H$ ) (J/g)
	Ti °C	Tf °C			
Calcite	771	831	32	3.65	28
China Clay	462	578	18	80.93	14
Talc	694	791	22	20	17
Whiting	771	840	50	-23	10

## V. CONCLUSION

In the current investigation, thermal decomposition of rock's minerals was studied with DSC in inert nitrogen atmosphere. It was found that decomposition proceeds through one and two stages of weight loss with detail of pyrolysis. The first stage is allocated to dehydration at around 600°C. In the second stage, the mass loss is a consequence of thermal decomposition of silicate minerals approximately 700°C with new layer-structure formation during the calcinations process was found as well as at high temperature the composition minerals was found stable. An endothermic and exothermic reaction process at certain temperature range, found in DSC analysis for all minerals. Heat capacity curve reveals enthalpy of fusion and enthalpy of crystallization.

## VI. ACKNOWLEDGMENT

The authors would like to gratefully acknowledge to Dr. K. R Patel (Physics Department, Sheth M N Science College, Patan, Gujarat, India) for providing a dedicated tools and thermal analysis techniques for quality analysis of the materials. We also show gratitude towards Gayatri minerals, GIDC, Mehsana, Gujarat, India for providing facility to obtain lumps of rock minerals from the various place of Rajasthan. Our sincere credit to Analytical Laboratory of CHARUSAT University, Changa, Gujarat, India for granting permission to use the required equipment for data for analysis.

## REFERENCES

- [1] Traore, K., Kabre, T. S., & Blanchart, P. (2003). Gehlenite and anorthite crystallisation from kaolinite and calcite mix. *Ceramics International*, 29(4), 377-383.

- [2] Leake, B. E. (1998). WA Deer, RA Howie and J. Zussman ISBN 1-897799-77-2. Mineralogical Magazine, 62(1), 135-136.
- [3] Alonso, M., Gonzalez, A., De Saja, J. A., & Escalona, A. M. (1991). Quality control of mineral impurities in industrial talcs by thermogravimetric analysis. *Thermochimica acta*, 184(1), 125-130.
- [4] Yang, N., Zhang, Z. C., Ma, N., Liu, H. L., Zhan, X. Q., Li, B., ... & Chiang, T. C. (2017). Effect of surface modified kaolin on properties of polypropylene grafted maleic anhydride. *Results in physics*, 7, 969-974.
- [5] Broido, A. (1969). *Journal of Polymer Science Part A-2: Polymer Physics*, 7(10), 1761-1773.
- [6] Simonsen, J. H., Poulsen, J. U., Rokkjaer, K. H., Christensen, L. H., Aasmul, S., & Iav, S. (2003). U.S. Patent No. 6,540,672.
- [7] Li, Q., He, R., Gao, J. A., Jensen, J. O., & Bjerrum, N. J. (2003). *Journal of the Electrochemical Society*, 150(12), A1599.
- [8] Ciullo, P. A. (1996). *Industrial minerals and their uses: a handbook and formulary*. William Andrew.
- [9] Murray, H. H. (2000). Traditional and new applications for kaolin, smectite, and palygorskite: a general overview. *Applied clay science*, 17(5-6), 207-221.
- [10] Guo, H., Qin, Z., Qian, P., Yu, P., Cui, S., & Wang, W. (2011). Crystallization of aragonite CaCO<sub>3</sub> with complex structures. *Advanced Powder Technology*, 22(6), 777-783.
- [11] Sunitrová, I., & Trník, A. (2018, July). DSC and TGA of a kaolin-based ceramics with zeolite addition during heating up to 1100° C. In *AIP Conference Proceedings* (Vol. 1988, No. 1, p. 020046). AIP Publishing LLC.
- [12] Ptáček, P., Kubátová, D., Havlica, J., Brandštetr, J., Šoukal, F., & Opravil, T. (2010). The non-isothermal kinetic analysis of the thermal decomposition of kaolinite by thermogravimetric analysis. *Powder Technology*, 204(2-3), 222-227.
- [13] Trivedi, M. K., Tallapragada, R. M., Branton, A., Trivedi, D., Nayak, G., Latiyal, O., & Jana, S. (2015). Physicochemical characterization of biofield energy treated calcium carbonate powder.
- [14] Horváth, E., Frost, R. L., Makó, É., Kristóf, J., & Cseh, T. (2003). Thermal treatment of mechanochemically activated kaolinite. *Thermochimica Acta*, 404(1-2), 227-234.
- [15] Pask, J. A., & Tomsia, A. P. (1991). Formation of mullite from sol-gel mixtures and kaolinite. *Journal of the American Ceramic Society*, 74(10), 2367-2373.
- [16] Peniche-Covas, C., Argüelles-Monal, W., & San Román, J. (1993). *Polymer Degradation and Stability*, 39(1), 21-28.
- [17] Mathew, A. P., Packirisamy, S., & Thomas, S. (2001). *Polymer Degradation and Stability*, 72(3), 423-439.
- [18] El-Sayed, S. A., & Mostafa, M. E. (2015). *Waste and Biomass Valorization*, 6(3), 401-415.
- [19] Chong, C. T., Mong, G. R., Ng, J. H., Chong, W. W. F., Ani, F. N., Lam, S. S., & Ong, H. C. (2019). *Energy Conversion and Management*, 180, 1260-1267.
- [20] Li, X. G., Lv, Y., Ma, B. G., Wang, W. Q., & Jian, S. W. (2017). *Arabian Journal of Chemistry*, 10, S2534-S2538.
- [21] Macêdo, R. O., Aragao, C. F. S., Do Nascimento, T. G., & Macêdo, A. M. C. (1999). *Journal of thermal analysis and calorimetry*, 56(3), 1323-1327.
- [22] Artiaga, R., Naya, S., Garcia, A., Barbadillo, F., & García, L. (2005). Subtracting the water effect from DSC curves by using simultaneous TGA data. *Thermochimica acta*, 428(1-2), 137-139.
- [23] Božanić, D. K., Djoković, V., Blanuša, J., Nair, P. S., Georges, M. K., & Radhakrishnan, T. (2007). Preparation and properties of nano-sized Ag and Ag<sub>2</sub>S particles in biopolymer matrix. *The European Physical Journal E*, 22(1), 51-59.
- [24] Gersten, J., Fainberg, V., Hetsroni, G., & Shindler, Y. (2000). Kinetic study of the thermal decomposition of polypropylene, oil shale, and their mixture. *Fuel*, 79(13), 1679-1686.
- [25] Tavangarian, F., Emadi, R., & Shafyei, A. (2010). Influence of mechanical activation and thermal treatment time on nanoparticle forsterite formation mechanism. *Powder technology*, 198(3), 412-416.
- [26] Willart, J. F., Carpentier, L., Danède, F., & Descamps, M. (2012). Solid-state vitrification of crystalline griseofulvin by mechanical milling. *Journal of pharmaceutical sciences*, 101(4), 1570-1577.
- [27] Mazumdar, S., & Mukherjee, B. (1983). Structural characterization of the spinel phase in the kaolin-mullite reaction series through lattice energy. *Journal of the American Ceramic Society*, 66(9), 610-612.
- [28] Krupka, K. M., Hemingway, B. S., Robie, R. A., & Kerrick, D. M. (1985). High-temperature heat capacities and derived thermodynamic

- properties of anthophyllite, diopside, dolomite, enstatite, bronzite, talc, tremolite and wollastonite. *American Mineralogist*, 70(3-4), 261-271.
- [29] Wesołowski, M. (1984). Thermal decomposition of talc: A review. *Thermochimica Acta*, 78(1-3), 395-421.
- [30] Stout, J. W., & Robie, R. A. (1963). Heat capacity from 11 to 300 K., entropy, and heat of formation of dolomite. *The Journal of Physical Chemistry*, 67(11), 2248-2252.
- [31] Dollimore, D., Tong, P., & Alexander, K. S. (1996). The kinetic interpretation of the decomposition of calcium carbonate by use of relationships other than the Arrhenius equation. *Thermochimica Acta*, 282, 13-27.
- [32] Cai, J., He, F., & Yao, F. (2007). Nonisothermal nth-order DAEM equation and its parametric study—use in the kinetic analysis of biomass pyrolysis. *Journal of mathematical chemistry*, 42(4), 949-956.
- [33] Venuvinod, P. K., & Lau, W. S. (1986). Estimation of rake temperatures in free oblique cutting. *International Journal of Machine Tool Design and Research*, 26(1), 1-14.
- [34] Likos, W. J., Olson, H. S., & Jaafar, R. (2012). Comparison of laboratory methods for measuring thermal conductivity of unsaturated soils. In *GeoCongress 2012: State of the Art and Practice in Geotechnical Engineering* (pp. 4366-4375).
- [35] Horai, K. I., & Simmons, G. (1969). Thermal conductivity of rock-forming minerals. *Earth and planetary science letters*, 6(5), 359-368.
- [36] Sprynskyy, M., Kowalkowski, T., Tutu, H., Cukrowska, E. M., & Buszewski, B. (2011). Adsorption performance of talc for uranium removal from aqueous solution. *Chemical Engineering Journal*, 171(3), 1185-1193.
- [37] Sprynskyy, M., Kowalkowski, T., Tutu, H., Cukrowska, E. M., & Buszewski, B. (2011). Adsorption performance of talc for uranium removal from aqueous solution. *Chemical Engineering Journal*, 171(3), 1185-1193.